Theoretical and experimental evidence indicates that there is no detectable auxin gradient in the angiosperm female gametophyte

Lituiev, Dmytro S ; Krohn, Nádia G ; Müller, Bruno ; Jackson, David ; Hellriegel, Barbara ; Dresselhaus, Thomas ; Grossniklaus, Ueli

Abstract: The plant life cycle alternates between a diploid sporophytic and a haploid gametophytic generation. The female gametophyte (FG) of flowering plants is typically formed through three syncytial mitoses, followed by cellularisation that forms seven cells belonging to four cell types. The specification of cell fates in the FG has been suggested to depend on positional information provided by an intrinsic auxin concentration gradient. The goal of this study was to develop mathematical models that explain the formation of this gradient in a syncytium. Two factors were proposed to contribute to the maintenance of the auxin gradient in Arabidopsis FGs: polar influx at early stages and localised auxin synthesis at later stages. However, no gradient could be generated using classical, one-dimensional theoretical models under these assumptions. Thus, we tested other hypotheses, including spatial confinement by the large central vacuole, background efflux and localised degradation, and investigated the robustness of cell specification under different parameters and assumptions. None of the models led to the generation of an auxin gradient that was steep enough to allow sufficiently robust patterning. This led us to re-examine the response to an auxin gradient in developing FGs using various auxin reporters, including a novel degron-based reporter system. In agreement with the predictions of our models, auxin responses were not detectable within the FG of Arabidopsis or maize, suggesting that the effects of manipulating auxin production and response on cell fate determination might be indirect.

DOI: https://doi.org/10.1242/dev.098301

© 2013. Published by The Company of Biologists Ltd | Development (2013) 140, 4544-4553 doi:10.1242/dev.098301

RESEARCH ARTICLE

Theoretical and experimental evidence indicates that there is no detectable auxin gradient in the angiosperm female gametophyte

Dmytro S. Lituiev[1], Nádia G. Krohn[2], Bruno Müller[1], David Jackson[3], Barbara Hellriegel[4], Thomas Dresselhaus[2] and Ueli Grossniklaus[1,*]

ABSTRACT

The plant life cycle alternates between a diploid sporophytic and a haploid gametophytic generation. The female gametophyte (FG) of flowering plants is typically formed through three syncytial mitoses, followed by cellularisation that forms seven cells belonging to four cell types. The specification of cell fates in the FG has been suggested to depend on positional information provided by an intrinsic auxin concentration gradient. The goal of this study was to develop mathematical models that explain the formation of this gradient in a syncytium. Two factors were proposed to contribute to the maintenance of the auxin gradient in *Arabidopsis* FGs: polar influx at early stages and localised auxin synthesis at later stages. However, no gradient could be generated using classical, one-dimensional theoretical models under these assumptions. Thus, we tested other hypotheses, including spatial confinement by the large central vacuole, background efflux and localised degradation, and investigated the robustness of cell specification under different parameters and assumptions. None of the models led to the generation of an auxin gradient that was steep enough to allow sufficiently robust patterning. This led us to re-examine the response to an auxin gradient in developing FGs using various auxin reporters, including a novel degron-based reporter system. In agreement with the predictions of our models, auxin responses were not detectable within the FG of *Arabidopsis* or maize, suggesting that the effects of manipulating auxin production and response on cell fate determination might be indirect.

KEY WORDS: *Arabidopsis*, Auxin, Female gametophyte, Gradient, Maize, Modelling

INTRODUCTION

The life cycle of plants alternates between a diploid sporophytic and a haploid gametophytic generation. In flowering plants, the sporophytic generation is the dominant form of the plant life cycle, whereas the gametophytic generation is highly reduced and short lived, and develops within the sexual organs of the flower.

In most flowering plants (70%), including *Arabidopsis thaliana* and *Zea mays* (maize), a postmeiotic female reproductive cell termed the functional megaspore (FM) undergoes three mitoses to form a female gametophyte (FG) comprising seven cells of four distinct cell types (Fig. 1).

[1]Institute of Plant Biology and Zürich-Basel Plant Science Center, University of Zürich, Zollikerstrasse 107, CH-8008 Zürich, Switzerland. [2]Cell Biology and Plant Biochemistry, Biochemie-Zentrum Regensburg, University of Regensburg, Universitätsstrasse 31, D-93053 Regensburg, Germany. [3]Cold Spring Harbor Laboratory, 1 Bungtown Road, Cold Spring Harbor, NY 11724, USA. [4]Anthropological Institute and Museum, University of Zürich, Winterthurerstrasse 190, CH-8057 Zürich, Switzerland.

*Author for correspondence (grossnik@botinst.uzh.ch)

Received 28 April 2013; Accepted 22 August 2013

In FG mutants with abnormally positioned or extra nuclei in maize (Evans, 2007; Srilunchang et al., 2010) and *Arabidopsis* (Gross-Hardt et al., 2007; Johnston et al., 2010; Moll et al., 2008; Pagnussat et al., 2007), the nuclei acquire their fate according to their spatial positioning along the micropylar-chalazal axis, suggesting that cell specification in the FG is driven by positional information. This hypothesis was strengthened by a microscopy study showing a graded activity of the auxin-sensitive reporter *DR5* (Ottenschläger et al., 2003) along the micropylar-chalazal axis of the FG (Pagnussat et al., 2009). Furthermore, overexpression of the auxin biosynthesis enzyme YUC1 and the artificial microRNA (amiRNA)-based knockdown of a group of auxin-dependent transcription factors (auxin response factors, ARFs) leads to the mis-specification of gametophytic cells (Pagnussat et al., 2009). Therefore, it was proposed that the phytohormone auxin is distributed in a gradient and serves as the morphogen driving cell specification in the *Arabidopsis* FG (Fig. 1) (Pagnussat et al., 2009; Sundaresan and Alandete-Saez, 2010).

Here, we attempted to reproduce the mechanisms of auxin gradient formation *in silico* for maize and *Arabidopsis* in order to verify whether the processes proposed previously, i.e. polar auxin influx at early stages and localised auxin synthesis at later stages (Pagnussat et al., 2009), are sufficient for the auxin gradient to be sustained, or whether additional factors should be considered. Using auxin degradation rates and diffusion coefficients from the literature, we found that only a very shallow auxin gradient can be maintained in *Arabidopsis* and a moderate one in maize, even if additional factors, such as background efflux or localised degradation, are incorporated into the model. Moreover, we showed that the steepness of the gradient obtained in our models does not allow a sufficiently robust cell fate acquisition, especially in the small *Arabidopsis* FG. Thus, we reanalysed the auxin response within ovules to refine our model. Surprisingly, we could not detect auxin-dependent *DR5* activity inside the FGs of either maize or *Arabidopsis* at any developmental stage. However, in both species we observed an auxin maximum in sporophytic nucellar cells at the micropylar pole of young ovules. As development progressed, *DR5* activity migrated towards the chalazal pole in the sporophytic tissues surrounding the FG. We propose a model involving non-cell-autonomous effects of auxin in the sporophytic tissues of the ovule, in which auxin overproduction in the FG can explain the cell fate changes observed by Pagnussat and colleagues (Pagnussat et al., 2009). Thus, auxin may affect cell specification indirectly through a function in sporophytic tissues rather than via a gradient in the FG.

RESULTS

Mathematical modelling shows that only shallow auxin gradients can be maintained in FGs

In order to elucidate potential mechanisms underlying the formation of an auxin gradient in angiosperm FGs, we developed a series of

Development (2013) doi:10.1242/dev.098301

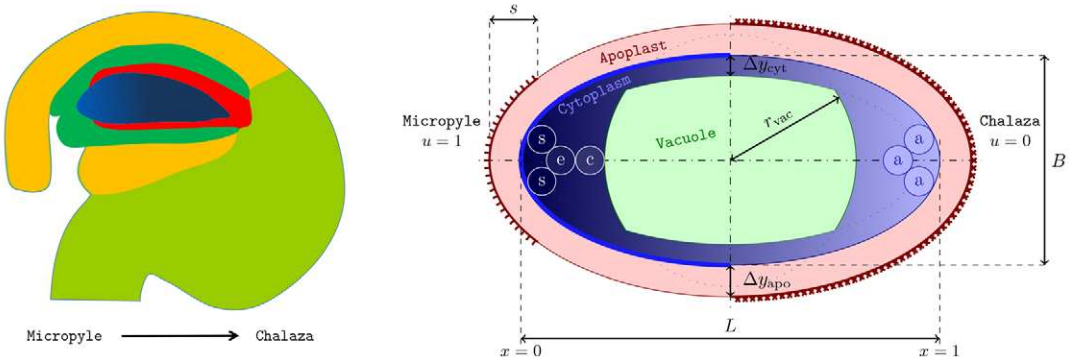

Fig. 1. Schematic representation of a FG. (Left) FG embedded in the context of the ovule. The endothelial tissue is shown in red, the inner integuments in green and the outer integuments in brown. (Right) Schematic of the FG showing features and geometrical parameters used in the simulations. An auxin gradient, which has been proposed to determine the cell fate of the synergids (s), egg cell (e), central cell (c) and antipodals (a), with decreasing concentration along the micropylar-chalazal axis is indicated in blue. The long axis of the FG from the micropylar (x=0) to the chalazal (x=1) pole is aligned with the x-axis in all models. The zone of auxin efflux is shown in dark-red pin lining. The zone where the concentration was set to zero is shown by dark-red x lining. The micropylar half of the plasma membrane where AUX1 was assumed to be expressed ≥5-fold higher than in the rest, is shown by a thick dark blue line. Not all proportions are preserved.

reaction-diffusion models based on the following assumptions: (1) auxin is produced or imported in the micropylar region of the FG; (2) auxin is degraded with first-order kinetics; and (3) diffusion of auxin is isotropic and homogenous throughout the cytoplasm.

We tested the contribution of different factor combinations (hereafter referred to as 'regimes') as described in Table 1. We included processes such as localised influx, both uniform and localised synthesis and degradation, as well as background efflux at the chalazal pole. As preliminary inspection showed that most parameter values produced only a very shallow gradient, we used parameter values that resulted in the steepest gradient, whenever alternative values were available from the literature (supplementary material Table S1).

PGP19 and AUX1 auxin carriers are expressed in the *Arabidopsis* FG

The distribution of auxin within plant tissues largely depends on polar auxin transport across membranes (reviewed by Garnett et al., 2010; Petrásek and Friml, 2009). Pagnussat and colleagues (Pagnussat et al., 2009) examined the expression of members of the PIN-FORMED (PIN) family of auxin transporters encoded by the *PIN1-4* and *PIN7* genes in the ovules and detected only PIN1 in the micropylar nucellar cells prior to the FG2 stage [all stages of FG development are given according to Christensen et al. (Christensen et al., 1997)]. Here, we further examined the expression of all other known auxin transporters in the FG. According to our RNA-Seq data, neither *PIN5* nor *PIN6* transcripts are detected in developing ovules (M. Schmid and U.G., unpublished). The PIN8 protein is not detected in ovules either (supplementary material Fig. S1), which is consistent with the fact that the *pin8-1* mutant is completely fertile (Dal Bosco et al., 2012).

In maize, we found ZmPIN1a-mRFP expression in sporophytic nucellar cells but not in the FG before the eight-nucleate stage (FG5), similar to previous findings in *Arabidopsis* (supplementary material Fig. S2; see also Fig. 7). In contrast to *Arabidopsis*, however, ZmPIN1a is expressed in the antipodal cells during FG maturation (stages FG6 and FG7). Because ZmPIN1a is expressed only at stages when the fate of the FG cells has already been determined, we did not consider this in our model.

The PGP1 (ABCB1) and PGP19 (ABCB19) efflux transporters are also known to participate in polar auxin transport (Geisler et al., 2005). Only PGP19 was found to be expressed in the *Arabidopsis* FG (supplementary material Figs S3, S4). The rates of PGP19-dependent and background auxin efflux used in our models were thus estimated based on earlier work by Geisler and colleagues (Geisler et al., 2005).

The AUXIN1/LIKE-AUX1 (AUX/LAX) family of transporters are known to facilitate auxin influx in *Arabidopsis* (Swarup and Péret, 2012). We found *AUX1* to be expressed in the *Arabidopsis* FG starting at the four-nucleate stage (FG4). Moreover, the protein accumulated in the micropylar part (supplementary material Fig. S5). Active auxin influx has been estimated to contribute up to 75% (Delbarre et al., 1996) of total auxin influx, with AUX1 contributing ~50% (Marchant et al., 1999), which was considered in our models. Close paralogs of *AUX1* with similar characteristics are either not detectable in the FG (*LAX3*) or are expressed at negligibly low levels (*LAX1* and *LAX2* at 2.2% and 1.0% of *AUX1* levels, respectively; M. Schmid and U.G., unpublished).

Table 1. Regimes used for the reaction-diffusion models

Parameter	Regime 1	Regime 2	Regime 3	Regime 4
Synthesis	None	Localised	None	None
Degradation	Uniform	Uniform	Localised	Uniform
Influx	Anterior pole	None	Anterior pole	Anterior pole
Efflux	None	None	None	Posterior pole

Measures of gradient steepness

As in most models of morphogen diffusion, our models were rescaled for analyses by combining the length of the FG, the diffusion coefficient, and the auxin degradation rate into a single parameter termed the characteristic length scale λ (Lander et al., 2009). However, as the models developed here account for boundary conditions relying on additional parameters, we could not use λ as a measure of the gradient steepness to compare different solutions. Therefore, we compared the different solutions based on a new measure termed the gradient steepness (GS), defined as the percentage by which the concentration drops towards the chalazal pole (u_{min}) from its maximum value (u_{max}) at the micropylar pole:

$$GS = \frac{u_{max} - u_{min}}{u_{max}} \cdot 100\% .$$

Development (2013) doi:10.1242/dev.098301

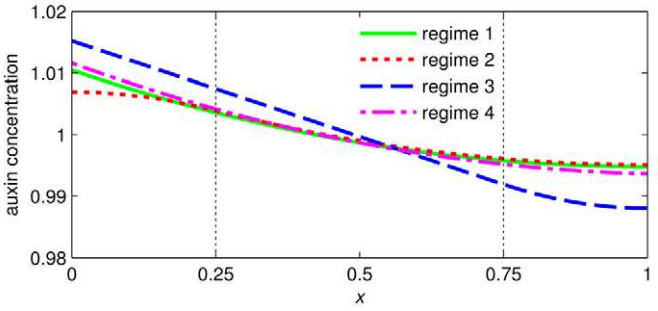

Fig. 2. Auxin concentration profiles in different regimes (one dimension) for *Arabidopsis*. The origin of the *x*-coordinate lies in the micropylar pole (*x*=0) and the axis runs towards the chalazal pole (*x*=1). Shaded areas represent the domains of localised synthesis (left) and degradation (right). Auxin concentration (*y*-coordinate) is presented in arbitrary units, assuming mean concentration = 1.

Simulation of the model in one dimension

Based on previous data indicating that the greatest variation in auxin concentration is observed along the micropylar-chalazal axis (Pagnussat et al., 2009), we studied a simplified one-dimensional model featuring spatial inhomogeneity of the processes along this axis. The spatial coordinate representing position along the micropylar-chalazal axis has its origin in the micropylar-most point (denoted as *x*=0) and spans the cytoplasm until the chalazal-most point (*x*=1) (Fig. 1). A numerical study of regime 1 (Table 1) in one dimension showed that the rate of auxin reaction-diffusion was much faster than the rate of FG growth, which allowed us to apply the quasi-steady state assumption with regard to reaction-diffusion (for details, see supplementary material Appendix S1). The absolute value of the error due to this simplification did not exceed 0.002% after 45 minutes of initial equilibration (supplementary material Fig. S6). Therefore, we focused on the eight-nucleate stage of FG development (FG5), when cell specification is believed to occur. At this stage, the FG of *Arabidopsis* reaches a length of up to 70 µm, whereas the maize FG is between 100 and 130 µm in the inbred line A188 (supplementary material Fig. S7).

The GS achieved under different regimes with parameter values obtained from the literature is shown in Fig. 2 and Table 2. Using regime 1 (localised influx and uniform degradation), a rather low GS of 0.78% was obtained for *Arabidopsis*; in maize, the GS reaches 2.66%. If we included local production of auxin at the micropylar pole instead of localised influx, as was suggested for late stages of FG development (Pagnussat et al., 2009), the simulation resulted in gradients that were even flatter than in the case of localised influx (Fig. 2, Table 2). By contrast, if we considered either localised degradation or background efflux of auxin, the steepness of the gradient increased (Figs 2, 4). Taken together, the simulations based on this one-dimensional model identified two factors capable of increasing GS compared with a result obtained with the simplest model (regime 1): background efflux producing a GS of 0.91% and 2.89% (regime 4) and localised degradation increasing the GS up to 1.36% and 4.55% (regime 3) in *Arabidopsis* and maize, respectively.

The large central vacuole can impede auxin diffusion in the FG, thereby increasing gradient steepness

At the two-nucleate stage (FG2), a large vacuole begins to form in the centre of the FG (Christensen et al., 1997; Schneitz et al., 1995; Huang and Sheridan, 1994). We investigated whether this vacuole can contribute to the maintenance of an auxin gradient in the FG by impeding the diffusion of auxin. To test this hypothesis, we set up a two-dimensional reaction-diffusion model with regimes 1 and 4, and solved it with the finite element method.

The results of this simulation showed that the large central vacuole will indeed impede diffusion, making the gradient steeper (Fig. 3, Table 2). This effect depends on the width of the cytoplasmic isthmus between the vacuolar and plasma membranes. Without the vacuole, two-dimensional models result in a GS that deviates less than 1% from that obtained with a one-dimensional model. However, with a width of the cytoplasmic isthmus of 1 µm, which is characteristic for *Arabidopsis* (supplementary material Fig. S8), the GS increases approximately two- to threefold in the two-dimensional model as compared with the model without a vacuole: from 1.33% to 3.21% in *Arabidopsis* and from 3.65% to 6.95% in maize (Fig. 4). In addition, taking localised AUX1-dependent influx into account, the GS decreases slightly by some thousandth of a percentage point (Fig. 4).

Thus, our simulations identify the effect of a vacuole together with carrier-dependent fluxes of auxin (by PGP19 and AUX1) as the most effective mechanisms that increase the steepness of a potential auxin gradient in the FG, leading to a GS of 3.21% and 6.95% in *Arabidopsis* and maize, respectively.

The theoretically achievable gradient of auxin cannot provide a sufficiently robust readout of positional information for cell specification

The morphogenetic signal providing positional information for cell specification can be corrupted by noise at different levels, both in its generation and perception (Lander et al., 2009). Perturbations of morphogen gradients can thus cause severe developmental aberrations and result in embryo lethality. Therefore, robustness is regarded as a major evolutionary constraint and is often used as an argument for or against the feasibility of theoretical models for morphogenetic gradients (e.g. Lander et al., 2009).

In order to theoretically assess the robustness of cell specification, we analysed the sensitivity of the theoretically achievable auxin gradient to perturbations in auxin concentration (for details see supplementary material Fig. S9 and Appendix S1). The auxin gradient obtained with physiological parameters is very shallow and makes the threshold position demarcating any two cell fate zones highly sensitive to perturbations in auxin concentration. A moderate perturbation of the auxin source by 3.5% leads to a positional shift of a given local auxin threshold throughout the entire length of the FG. Even a very small change of 0.5% in the auxin source leads to a shift of the threshold of at least 20%, which, for instance, is sufficient to disrupt cell specification in the micropylar part of the FG (Fig. 5; supplementary material Table S2). By contrast, a perturbation of the *Drosophila* Bicoid (Bcd)

Table 2. Gradient steepness (%) under different regimes

Species	Regime 1, 1D	Regime 2, 1D	Regime 3, 1D	Regime 4, 1D	Regime 4, 2D, evenly distributed AUX1, no vacuole	Regime 4, 2D, evenly distributed AUX1, with vacuole	Regime 4, 2D, polar AUX1, with vacuole
Arabidopsis	0.783	0.588	1.361	0.909	1.328	3.213	3.207
Maize	2.658	2.004	4.550	2.885	3.647	6.947	6.945

Development (2013) doi:10.1242/dev.098301

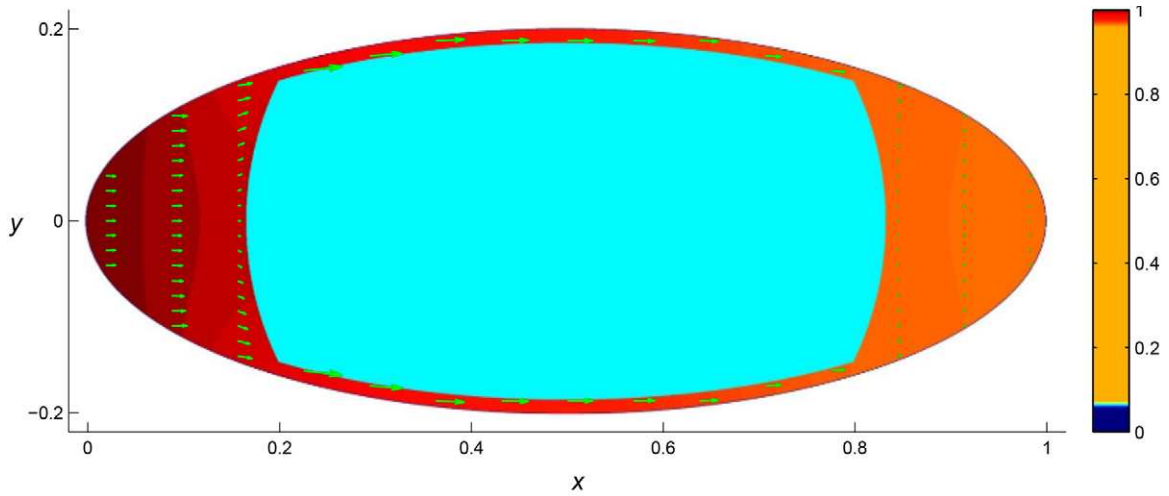

Fig. 3. Simulation result of the two-dimensional model in regime 4. Total auxin concentration is shown by colour code and auxin flux is indicated by green arrows (the length indicates flux intensity in logarithmic scale, arbitrary units). Note the maximal flux inside the cytoplasm is observed in the cytoplasmic isthmuses around the central vacuole. The colour code (right) is specially adjusted to emphasize the gradient.

gradient by 5% results in changes in the perceived position of less than 5% in the region where the positional information is read out under all parameters tested (de Lachapelle and Bergmann, 2010). Therefore, the theoretical auxin gradient in the FG is extremely sensitive to perturbations compared with the well-studied *Drosophila* Bcd gradient and is thus highly unlikely to provide the stable positional information required for cell specification.

In summary, the auxin gradient obtained with known, realistic parameters is very sensitive to variation in the auxin source and thus would make cell specification highly unreliable. This result can be interpreted as follows: (1) the rate of auxin diffusion or background efflux in the FG is drastically different from that in all other known cases, which is very unlikely; (2) additional factors, for instance efflux mediated by as yet unknown transporters, contribute to the maintenance of the gradient; or (3) the auxin gradient achieved under these realistic conditions is not sufficient, or provides only part of the positional information needed, for cell fate determination; for instance, auxin might be a trigger of polarisation but not provide the positional information required for cell specification.

Microscopy analyses of auxin activity in *Arabidopsis* and maize ovules reveal no auxin activity inside the FG

Our modelling results predicted only very shallow auxin gradients using known, realistic parameters in *Arabidopsis* and, to a lesser extent, in maize. To test this prediction, we aimed to characterise auxin activity in the ovule and FG experimentally in both *Arabidopsis* and maize using the classical *DR5* auxin-sensitive promoter (Ulmasov et al., 1997) and novel reporters based on auxin-dependent protein degradation.

Auxin response in ovules of *Arabidopsis thaliana*

Three different *DR5* lines were studied, each harbouring a different fluorescent protein: an endoplasmic reticulum (ER)-targeted GFP (Ottenschläger et al., 2003), a nuclear-targeted triple GFP (Weijers et al., 2006), and a nuclear localised tandem Tomato (tdTomato) fluorescent protein; the latter line additionally carried a nuclear YFP expressed under the gametophyte-specific *AKV* promoter (Rotman et al., 2005), marking all gametophytic nuclei. All three lines displayed the same pattern of *DR5* activity. At the megaspore mother cell (MMC) stage (Fig. 6A,F,K), *DR5* activity was observed in cells of the L1 and sometimes L2 layer of the nucellus surrounding the MMC, mostly at the future micropylar pole. Later, at the FM stage (FG1, Fig. 6B,G,L), the highest *DR5* activity was observed in the micropylar region of the nucellus in cells of the L1 and L2 layer, with some activity in the L2 cells surrounding the FM laterally. At the early two-nucleate stage of FG development (FG2, Fig. 6C,H,M), the pattern remained largely the same; however, the FG begins to displace the nucellar tissue (Schneitz et al., 1995) and, in the late two-nucleate stage (FG3, Fig. 6D,I,N), at its micropylar pole the FG comes into contact with the inner integuments, which lack *DR5* expression. At the four-nucleate stage (FG4, Fig. 6E,J,O), most of the nucellar tissue

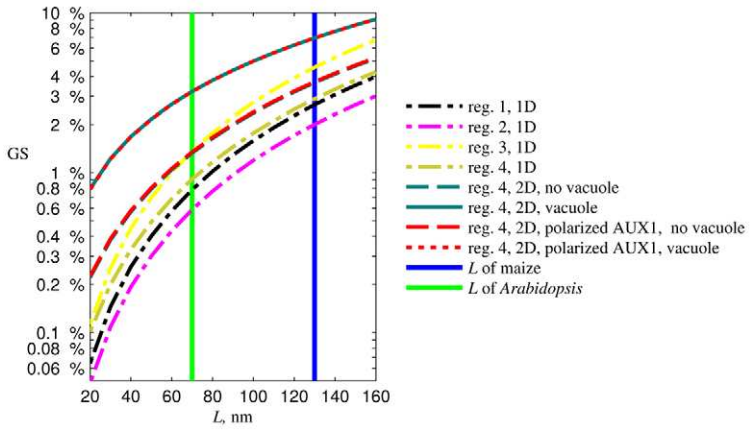

Fig. 4. Dependence of the gradient steepness on the length *L* of the FG for different model modifications. Localised synthesis (regime 2) is assumed to occur in the 1/4 micropylar-most part, whereas localised degradation (regime 3) is assumed to occur in the 1/4 chalazal-most part of the FG. The FG sizes (*L*) for *Arabidopsis* and maize at stage FG5 are indicated by vertical lines. Regime 4 in two dimensions results in maximal gradient steepness, especially when a vacuole is included. Addition of AUX1 to the model in regime 4 (2 dimensions) results in only a very minor increase in the gradient steepness. In maize, due to the larger size of the FG, steeper gradients can be achieved.

Development (2013) doi:10.1242/dev.098301

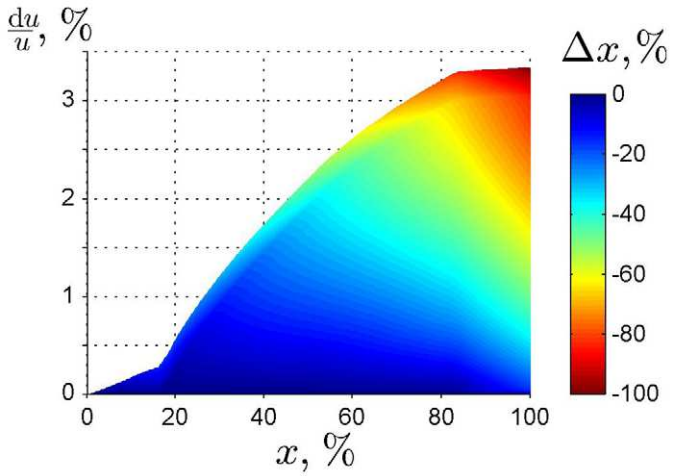

Fig. 5. The theoretically achievable auxin gradient is highly sensitive to noise in the auxin concentration. The value of the predicted positional variability of the threshold position as a response to a perturbation in the auxin concentration (equivalent to a shift in source intensity) in percentage of the length of the FG is indicated in colour code. The blank space represents the positions where the perturbation shifts the perceived threshold position out of the domain boundaries (i.e. no cells in the FG can achieve the cell fate determined left of the corresponding threshold position anymore). Note that a perturbation of ~0.51% disrupts cell specification in the micropylar part of the FG (x<0.2) and any perturbation higher than 3.5% disrupts it in the entire FG.

in the micropylar and medial part has degenerated and *DR5* activity is concentrated in the nucellar tissue adjacent to the chalazal pole of the FG. Later, at the final developmental stages (FG5 and FG6), some sporophytic cells adjacent to the chalazal pole of the FG were found to express *DR5* (supplementary material Fig. S10). From the four-nucleate until the final stages, a single *DR5*-expressing cell can be seen at the micropylar tip of the inner integument in fewer than a quarter of the ovules.

To obtain an alternative auxin signalling readout, we developed transgenic plants carrying a novel degron-GFP sensor, which exploits the auxin-dependent degradation of AUX/IAA proteins. Auxin binding to the ubiquitin ligase TRANSPORT INHIBITOR RESPONSE1 (TIR1) causes the degradation of AUX/IAA proteins via their domain II (Ramos et al., 2001). We used the six amino acid domain II core VGWPPV peptide, which is common to more than 70% of AUX/IAA isoforms (Ramos et al., 2001), as a C-terminal fusion to GFP6. An analogous reporter, DII-Venus, was developed in parallel (Vernoux et al., 2011) but is driven by the *35S* promoter, which is thought to be inactive in the FG (Desfeux et al., 2000) (U.G., unpublished) and was not detected in the FG (supplementary material Fig. S11). By contrast, a bright signal of degron-GFP driven by the ubiquitin 10 (*UBQ10*) promoter (*pUBQ10*) is visible throughout FG development (Fig. 6P-T), indicating that there is not a sufficiently high auxin concentration to cause degradation of the reporter. Although degron-GFP levels during the initial stages of ovule development are lower in sporophytic tissues than in the developing FG, an even lower level was detected in nucellar cells that express *DR5* (Fig. 6P,Q). Thus, the pattern of auxin activity inferred from degron-GFP is complementary to the pattern displayed by the *DR5* promoter. Thus, even though the dynamic range of degron-GFP activity apparently lies in a lower range of concentrations than that of *DR5*-driven fluorescent proteins, the qualitative patterns displayed by both are consistent.

We observed lower levels of degron-GFP in many sporophytic cells than in the FG, even though neither displayed *DR5* activity. This prompted us to test whether *pUBQ10* showed differential activity in these cells and to use a control pUBQ10::GFP line to estimate relative auxin levels. A comparison of fluorescence intensities between pUBQ10::degron-GFP and control pUBQ10::GFP lines allowed us to correct for inhomogeneities in the protein levels due to differences in promoter activity. Accounting for these corrections, degradation of degron-GFP is significantly higher in the nucellar cells surrounding the FG than in the FG at both the FM (FG1) and late two-nucleate (FG3) stages (supplementary material Fig. S12, Table S3), which is in agreement with the pattern displayed by the *DR5* promoter.

In conclusion, we could not detect any auxin activity inside the *Arabidopsis* FG experimentally. On the contrary, we found that until the late two-nucleate stage (FG3) the ovule's minimum auxin activity is localised in the FG. Moreover, the pattern of auxin activity in the sporophytic nucellus tissue is highly dynamic and exhibits the following features: (1) an auxin maximum usually in the two epidermal cells (L1 layer) at the tip of the ovule as the MMC differentiates in the L2 layer; (2) migration of the *DR5* activity maximum from the micropylar towards the chalazal pole; and (3) degeneration of *DR5*-expressing cells in the micropylar region of the nucellus.

Auxin response in ovules of *Zea mays*

In maize, we studied the expression pattern of *DR5* driving an ER-targeted red fluorescent protein (mRFP:ER) (Gallavotti et al., 2008). As shown in Fig. 7A, a strong *DR5* signal was visible at the tip of an ovule primordium in a few epidermal cells of the L1 layer in immediate proximity to a subepidermal cell of the L2 layer that differentiates into the MMC. The auxin response expanded around this cell, which enlarges at its micropylar pole and elongates longitudinally, and which appears smaller towards its chalazal pole (Fig. 7B,C). The nucleus of the emerging, highly polarised MMC moved towards the micropylar pole close to the auxin maximum, and initiated meiosis. After completion of meiosis, the three micropylar-most megaspores degenerated and the FM (FG1) became more deeply embedded into the L3 layer of the developing ovule (Fig. 7D-F).

Although the cells showing *DR5* activity at the tip of the ovule expanded to the L2 layer, these sporophytic auxin-responsive cells were no longer neighbouring the FG after the FG1 stage. During FG development, *DR5* activity decreased, beginning at stage FG2 (Fig. 7G-I), and was no longer detectable in micropylar nucellar cells from stage FG5 onwards (Fig. 7J). In mature ovules, *DR5* activity was entirely absent from this region at stage FG7 (Fig. 7K,L; supplementary material Fig. S13). By contrast, a strong *DR5* signal became visible in the tips of the inner and outer integuments (Fig. 7J; supplementary material Fig. S13A,B), as well in the gametophytic antipodal cells, with the strongest signals in the antipodal cells located furthest from the central cell (Fig. 7K,L; supplementary material Fig. S13C,D).

In conclusion, *DR5* activity, and thus a nuclear auxin response gradient, was not observed inside the developing FG of maize before the completion of cellularisation at stage FG6, by which time cell specification has presumably already taken place. The only gametophytic *DR5* signal was observed in the antipodal cells, after cellularisation and during their proliferation.

Sporophytic non-cell-autonomous effects may explain cell fate changes in the FG

Our theoretical results suggested that, with known parameters, an auxin gradient cannot be maintained in the FG, and our experimental

Development (2013) doi:10.1242/dev.098301

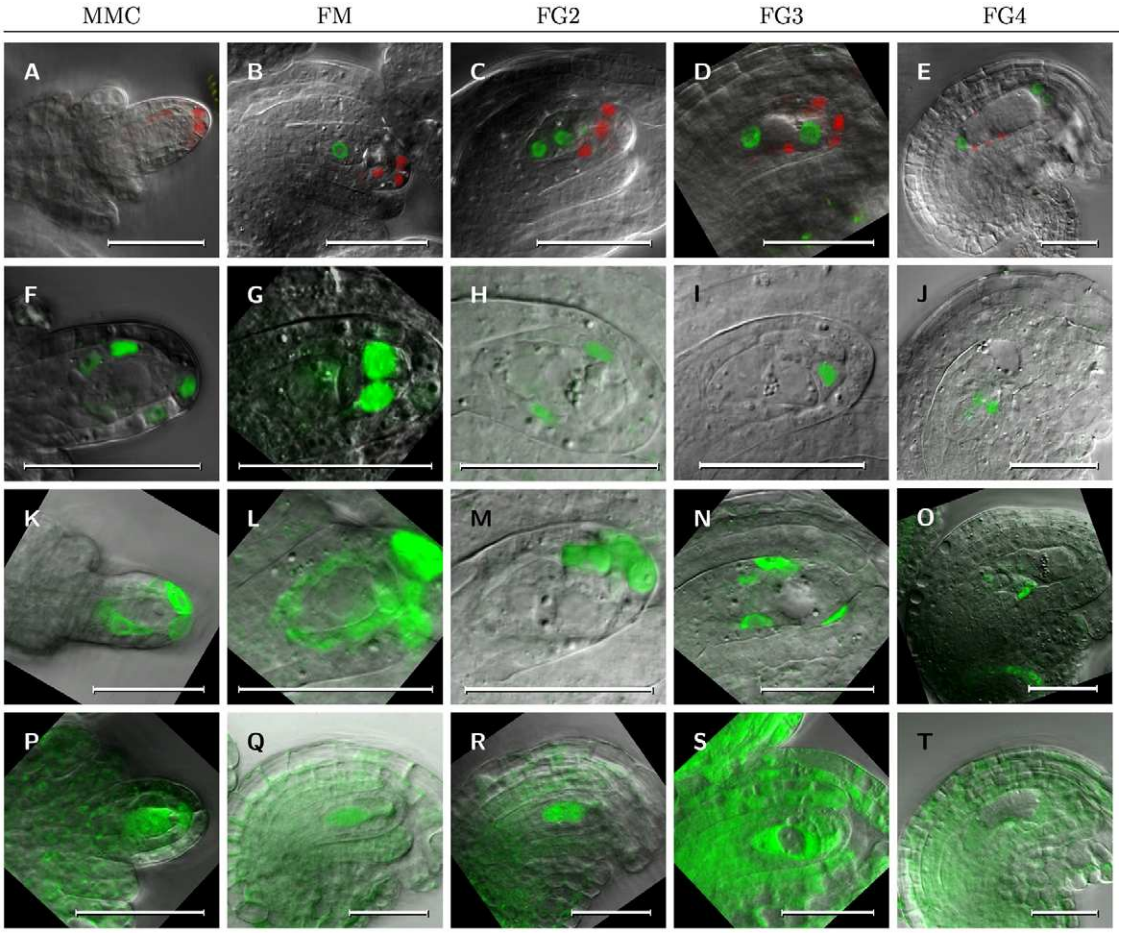

Fig. 6. Auxin response in *Arabidopsis* ovules during FG development. Stages of ovule development using four independent auxin reporter lines (see text for details). The following stages are shown: megaspore mother cell (MMC), functional megaspore (FM, also referred to as FG1), two-nucleate FG (FG2), two-nucleate FG with large central vacuole (FG3) and four-nucleate FG (FG4). (A-E) DR5::Dof1a:tdTomato (red) line with the AKV::H2B:YFP gametophytic fate marker (green); (F-J) DR5::SV40:3×GFP; (K-O) DR5::GFP-ER; (P-T) pUBQ10::degron-GFP. The images are oriented such that the micropylar pole of the ovules points to the right. At the MMC (A,F,K,P), FM (B,G,L,Q) and FG2 (C,H,M,R) stages auxin activity is observed only in cells surrounding the MMC or FG. At early stages, the maximum auxin activity is in the epidermal cells at the very micropylar tip of the ovule; later, also sporophytic cells in lateral regions of the nucellus show high auxin activity. At the FG2 stage (D,I,N,S) the nucellar tissue surrounding the FG begins to degenerate, starting at the micropylar pole. Some lateral sporophytic cells show auxin activity. At the FG4 stage (E,J,O,T) the surrounding nucellar tissue continues to degenerate; cells with a maximum in auxin activity are found more towards the chalazal pole. Throughout its development, no auxin activity can be observed within the FG (note that there is no overlap of the green gametophytic cell fate marker with the red DR5-driven fluorescent protein in the top row). Scale bars: 30 μm.

data showed that indeed no auxin activity can be detected inside the FGs of *Arabidopsis* and maize. However, earlier experiments had shown that auxin overproduction in the *Arabidopsis* FG can lead to changes in the fate of gametophytic nuclei (Pagnussat et al., 2009). Based on the results presented here, this change in cell fate does not come about by altering the auxin gradient inside the FG as previously interpreted. Here, we suggest an alternative hypothesis that can explain such changes through effects of auxin overproduction in the FG on the surrounding sporophytic tissues. Given that there is no detectable auxin gradient in the FG but that (1) there is polarised auxin activity in the sporophyte and (2) there are effects of auxin overproduction on gametophytic cell specification, it is likely that auxin has some effect in sporophytic tissues that indirectly affects cell fate decisions in the FG, namely via a non-cell-autonomous signal (NCAS).

To examine whether such a scenario could explain the experimental observations made by Pagnussat and colleagues (Pagnussat et al., 2009), we used as a basis the two-dimensional steady state model with a vacuole described above. We developed a mathematical model that is based on the assumption that the promoter of NCAS is responsive to auxin in sporophytic cells. Auxin leads to its activation in an all-or-none manner, i.e. the promoter becomes active if the concentration of auxin exceeds a certain threshold concentration c_{thr}. This serves as a good approximation for a more realistic scenario using a Hill activation function (e.g. Alon, 2007). The NCAS diffuses throughout the domain and is degraded inside the cells with the rate a_{NCAS}. For simplicity, we assumed that its diffusion coefficient in the membrane has the same value as in the cytoplasm (D_{NCAS}) (see supplementary material Table S4 for the values of parameters used).

Using this model, we studied the impact of auxin overproduction inside the FG on the spatial distribution of the NCAS. The concentration of auxin, the activity of the NCAS promoter, and the concentration of NCAS itself are visualised in Fig. 8 under different levels of auxin synthesis. It is obvious that, depending on the level of auxin production in the FG (and the promoter activation threshold; data not shown), different spatial distributions of the NCAS can be achieved. In fact, high levels of auxin production lead

Development (2013) doi:10.1242/dev.098301

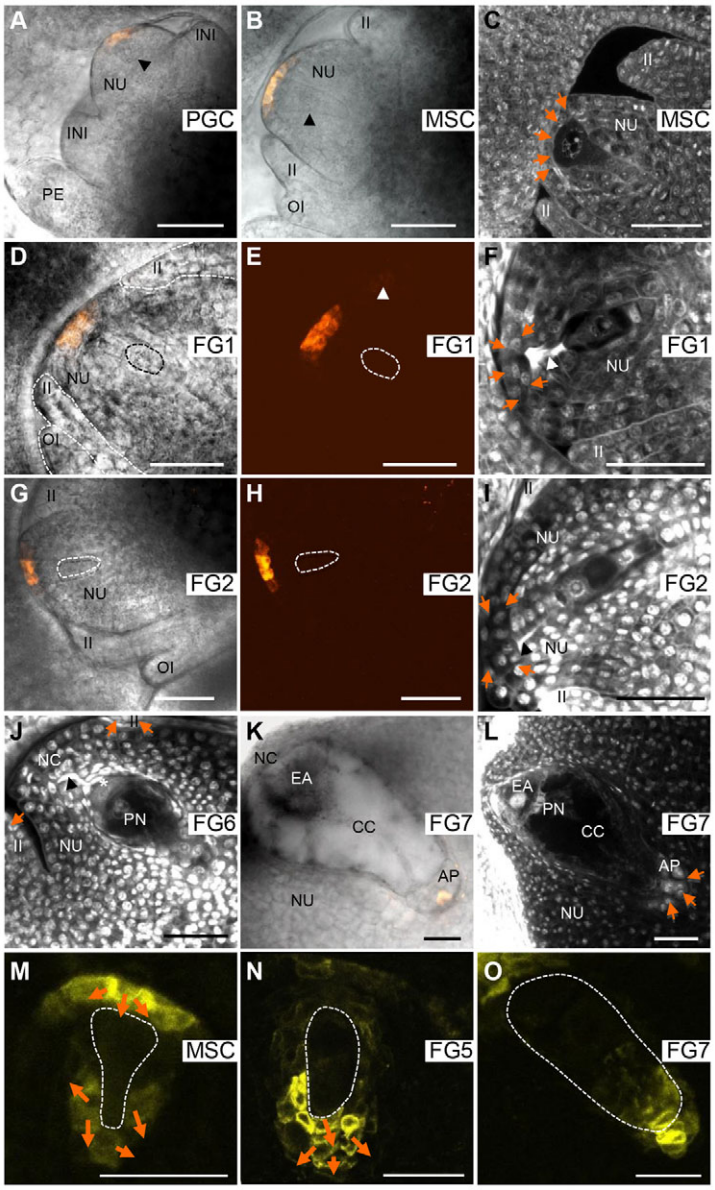

Fig. 7. Auxin response and flux in the maize ovule during female germline development. DR5::mRFP:ER (A-L) and ZmPIN1a::PIN1a:YFP (M-O). Developmental stages are indicated in each panel. (A) A subepidermal L2 nucellar cell in immediate proximity to strongest *DR5* reporter expression in L1 differentiates into the primordial germ cell (PGC; arrowhead). (B) The PMC has differentiated into a highly polar MMC (arrowhead). (C) Section through the ovule at MMC stage. MMC is in pachytene stage of meiosis I. Arrows point towards a single L1 nucellus cell layer displaying a strong auxin response in B. (D,E) *DR5* expression after meiosis at stage FG1. Three megaspores degrade and the FM is encircled. *DR5* activity expands to the L2 micropylar nucellus. Arrowhead in E indicates the L1 layer. (F) Section through the ovule at stage FG1. Remnants of degenerated megaspores are indicated by an arrowhead. Arrows point towards L1 and L2 nucellar cells showing a strong auxin response in fluorescent images. (G,H) Stage FG2. The FG is indicated by the white dashed line. (I) Ovule at stage FG2. Remnants of degenerated megaspores are indicated by an arrowhead and nucellar cells showing an auxin response in fluorescent images are indicated by arrows. (J) Ovule at stage FG6. Cellularisation of the FG has completed. The egg cell nucleus is located below the asterisk. Arrowhead indicates remnants of degenerated megaspores and arrows indicate an auxin response in integument tips of fluorescent images. (K) Mature FG containing more than 20 antipodal cells. Integuments were removed. (L) Section through the ovule at mature stage FG7. Antipodal cells showing an auxin response are indicated by arrows. (M) Auxin flux in L1 micropylar nucellar cells points towards the highly polar MMC (outlined by dashed line), but is depleted at its chalazal pole. (N) At stage FG5, ZmPIN1a is visible at high levels in nucellar cells surrounding the chalazal pole of the FG. (O) At stage FG6 ZmPIN1a is expressed inside antipodal cells. (A,B,D,K) Merged brightfield und epifluorescent images. (E,H) Fluorescence images of D and G, respectively. (C,F,I,J,L) Stack of confocal sections of fixed ovules. (M-O) Fluorescent images of ZmPIN1a-expressing ovules. Orange arrows indicate the cells showing a strong auxin response, as shown by DR5 expression. AP, antipodal cells; CC, central cell; EA, egg apparatus; II, inner integument; INI, integument initials; NC, nucellar cap; NU, nucellus; OI, outer integument; PE, pericarp; PN, polar nuclei. Scale bars: 50 μm.

to a complete loss of polarity in the spatial distribution of NCAS (Fig. 8), which is expected to result in cell fate changes.

In summary, the changes in nuclear fate observed upon auxin overproduction inside the FG can be explained by auxin flux into the surrounding sporophytic tissues. This will lead to an expansion of the auxin response beyond the area seen in wild-type ovules at the chalazal pole and may have indirect effects on cell specification inside the FG.

DISCUSSION

Our modelling results show that even under the most beneficial parameters and assumptions, the concentration of auxin drops from one end of the FG to the other only by 3.2% and 6.9% in *Arabidopsis* and maize, respectively. This is much lower than, for instance, the steepness of the Bcd gradient in *Drosophila*, which is more than 90% (Gregor et al., 2005; He et al., 2010). We found that such a shallow gradient is highly sensitive to perturbations in the auxin source, and perturbations of 3.5% or more in the auxin source completely disrupted patterning in the FG, whereas for the Bcd gradient such perturbations would lead to a shift of the threshold position of merely 4%. Therefore, such a shallow gradient would compromise the robustness of cell specification with regard to the various fluctuations that are inherent to biological systems, especially in the intensity of the auxin source. We conclude that the factors studied do not allow the production of a sufficiently steep auxin gradient to provide enough positional information for cell specification in the FG. This led us to an attempt to quantify *DR5* activity in the FG in order to refine the model.

Unexpectedly, our microscopy studies showed that, in contrast to a previous report (Pagnussat et al., 2009), auxin-dependent activity cannot be detected inside developing FGs in *Arabidopsis* or maize. Additionally, we found that the pattern of auxin activity in sporophytic cells adjacent to the FG is highly dynamic. The most notable developmental change in the pattern of auxin activity in the *Arabidopsis* ovule is the progressive movement of auxin maxima in cells adjacent to the developing FG from the micropylar towards the chalazal pole. It is tempting to speculate that this polarised activity could trigger indirect, non-cell-autonomous effects that influence cell specification inside the FG. Similarly, in maize, auxin activity was not observed inside the FG until cellularisation was complete.

Development (2013) doi:10.1242/dev.098301

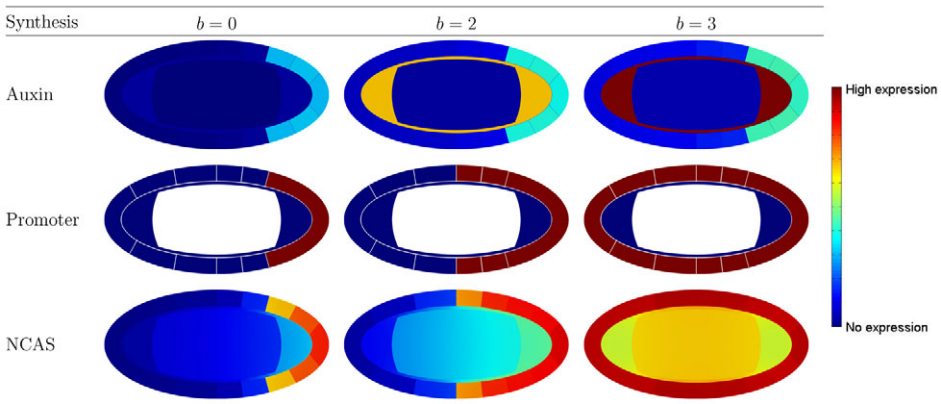

Fig. 8. Overproduction of auxin in the FG can lead to expansion of a auxin-induced non-cell-autonomous signal in the sporophyte and loss of polarity. Expression of auxin is shown in a heat map colour code. The FG is oriented such that the micropylar pole is on the left. Different levels of auxin expression (*b*=0, 2, 3) are represented in the three columns: the first column represents a situation when no auxin is synthesized in the FG, whereas the following two columns show increasing levels of auxin expression inside the FG, which ultimately leads to a loss of polarity in the sporophytic tissues surrounding the FG. See text for details.

Instead, auxin activity was detected in adjacent sporophytic nucellar cells of the micropylar pole at early stages and in proliferating antipodal cells during FG maturation. A similar pattern has recently been described in *Hieracium pilosella*, in which no evidence for *DR5* activity inside the FG was found (Tucker et al., 2012).

Taken together, our theoretical and experimental studies are inconsistent with the earlier report of a graded auxin-dependent activity in the FG of *Arabidopsis* (Pagnussat et al., 2009). This gives us reason to believe that these earlier results were misinterpreted and that the area with *DR5* activity assigned to the FG in fact encompassed a larger area including sporophytic cells in the nucellus, which indeed express DR5::GFP-ER. The exact boundary of the FG might not be easily identifiable by epifluorescence microscopy, as used in the previous study (Pagnussat et al., 2009), but is very clear under a confocal laser-scanning microscope and, especially, with nuclear localised reporters (Fig. 6A-J).

However, the experimental manipulations of auxin synthesis (by *YUC1* overexpression) and signalling (amiRNA-mediated knockdown of ARFs) in the FG that perturbed gametophytic cell fate seemed consistent with the hypothesis of an auxin gradient (Pagnussat et al., 2009) and warrant an explanation. Here, we propose hypotheses that are consistent with the effects on cell specification observed in these studies. First, changes in the fate of gametophytic nuclei can be explained by sporophytic effects of auxin overproduction in the FG. Using a modelling approach, we showed that auxin overproduction can indeed lead to a breakdown of polarity and loss of positional information inside the FG that results from auxin leakage into sporophytic tissues. In fact, our theoretical results agree with previous observations that showed an expansion of *DR5* activity into the surrounding sporophytic tissues upon *YUC1* overexpression [figure S5 in Pagnussat et al. (Pagnussat et al., 2009)]. Such an effect would be mediated by a hypothetical auxin-dependent NCAS, which is produced in sporophytic cells and controls cell specification in the FG. For instance, the peptide ZmEAL1 secreted from the egg cell has recently been shown to regulate cell fate within the maize FG in a non-cell-autonomous manner (Krohn et al., 2012). Similarly, peptides controlling cell fate in the FG could be secreted by surrounding nucellar cells.

Second, the effects observed by Pagnussat and colleagues (Pagnussat et al., 2009) could be mediated by some auxin-independent components of auxin signalling in the FG. For example, the transcription factors ARF3 and ARF17 possess auxin-like activity but are uncoupled from auxin signalling (Guilfoyle and Hagen, 2007). Both are transcribed in the central cell (Schmid et al., 2012) and show polarised mRNA expression in FGs at the four-nucleate stage (M. Schmid and U.G., unpublished). Downregulation of one of these factors, such as ARF3 in the experiment described by Pagnussat and colleagues (Pagnussat et al., 2009), would reduce such an auxin-independent auxin-like signal, whereas auxin overproduction would mask effects of ARF3 and/or ARF17 expression. Nevertheless, the activity of ARF3 or ARF17 should theoretically be detectable by the *DR5* sensor; the fact that *DR5* activity is not observed in the FG could mean that this activity is below the threshold of detection.

Finally, there could be minimal auxin-dependent activity in the FG that is below the detection level of any of our reporter systems with a very shallow gradient. Even though our modelling has shown that this gradient cannot provide positional information that is sufficiently robust for cell specification, it could determine the polarity of another morphogen through so-called wave-pinning (Mori et al., 2008). Such a model depends on two interconverting molecular species, whereby a progressing but eventually decelerating activation wave of one species would be initiated at one pole of the FG, leading to the depletion of the second species in this process. Thus, wave pinning could convert a spatially more or less homogeneous concentration profile into an asymmetric stationary front profile. However, wave pinning crucially depends on very different rates of diffusion of the two species, with the active form having the low diffusion rate. For instance, the interconversion of membrane-bound and a soluble forms of Rho GTPases can polarize cells by wave-pinning (Mori et al., 2008). Auxin is known to activate the ROP2 and ROP6 Rho GTPases in *Arabidopsis* epidermal cells through a yet poorly understood transcription-independent auxin signalling pathway (Xu et al., 2010). However, it is unknown whether Rho GTPases play a role in FG development or whether any other signaling molecules in the FG fulfil the requirements for wave pinning, i.e. rapid interconversion and highly different diffusion rates.

Although alternative explanations for the outcome of the experiments perturbing auxin production and signalling can be provided, there are currently not enough data to suggest a more precise mechanism. In particular, the most frequent cell fate change observed in both auxin overproduction and ARF amiRNA knockdown experiments was a loss of cell fate marker expression, whereas misexpression of egg and synergid cell markers was rather rare (Pagnussat et al., 2009). Thus, additional experiments that allow a more precise manipulation of auxin and/or other factors within and outside the FG will be required to develop accurate models of cell specification in the FG. In conclusion, neither our theoretical nor experimental evidence supports the hypothesis that a gradient in auxin activity provides the positional information for cell specification in the FG of flowering plants.

MATERIALS AND METHODS

Mathematical simulations

One-dimensional solutions were found analytically and were simulated in MATLAB 2011b software (MathWorks, Natick, MA, USA) using the *pdepe* function. Two-dimensional simulations were carried out with COMSOL Multiphysics 4.3a software (COMSOL Group, Stockholm, Sweden), exploiting the finite element method. To study the robustness of patterning, one-dimensional data or one-dimensional averages of two-dimensional simulations were used. Details are provided in supplementary material Appendix S1 and Tables S1, S4 and S5.

Generation of transgenic constructs

The DR5::NLS:tdTomato plasmid was constructed using a 35Smin:TMVΩ:Dof1a:tdTomato vector (B.M., unpublished), which is derived from a pCB302 binary vector (Xiang et al., 1999), carrying the TMVΩ translational enhancer (Gallie, 2002) and the Dof1a nuclear localisation signal (NLS) (Yanagisawa and Sheen, 1998) translationally fused to the tdTomato fluorescent protein gene (Shaner et al., 2004). The PCR-amplified *DR5* synthetic promoter from the DR5::GFP-ER plasmid (Ottenschläger et al., 2003) was inserted into the Ω:Dof1a:tdTomato vector.

The pUBQ10::degron:GFP plasmid was obtained by inserting a sequence encoding the degron consensus core of AUX/IAA proteins (VGWPPV) into the pMDC111 vector (Curtis and Grossniklaus, 2003) with subsequent Gateway insertion of the 2.5 kb *Arabidopsis* ubiquitin *UBQ10* promoter as explained in supplementary material Fig. S14. The control pUBQ10::GFP construct was obtained similarly. The constructs were verified by sequencing.

Plant material and growth conditions

The *Arabidopsis* DR5::GFP:ER line (Ottenschläger et al., 2003) was obtained from Jiří Friml (Flanders Institute of Biotechnology, Belgium), DR5::SV40:3×GFP (Weijers et al., 2006) from Dolf Weijers (Wageningen University, The Netherlands), and the DR5::NLS:tdTomato line is described here for the first time (see above). The PGP1::PGP1:GFP line in a *pgp1* homozygous background, the PGP19::PGP19:GFP line in a *pgp19* homozygous background (Geisler et al., 2005), and the AUX1::AUX1:YFP line in a *aux1-22* homozygous background (Swarup et al.,. 2004) were provided by Markus Geisler (Université de Fribourg, Switzerland); the PIN8::PIN8:GFP line (Dal Bosco et al., 2012) was provided by Cristina Dal Bosco (Albert-Ludwigs-Universität Freiburg, Germany). Unless indicated otherwise, all plants used were *Arabidopsis thaliana* (L.) Heynh. var. Columbia-0 (Col-0).

DR5::NLS:tdTomato transformants were obtained by *Agrobacterium*-mediated floral dip transformation (Bent, 2006). Seven independent transformants were recovered from BASTA selection and microscopically screened for tdTomato expression in ovules in the T1 (heterozygous plants) and T3 (homozygous plants) generations; a qualitative variation in expression patterns among the seven independent lines was not observed. A representative DR5::NLS:tdTomato line was crossed with the AKV::H2B:YFP gametophytic fate marker line (Rotman et al., 2005), provided by Wei-Cai Yang (Chinese Academy of Science, Beijing, China), which is in the Landsberg (*erecta* mutant, L*er*) background, and F3 plants homozygous for both constructs were analysed.

Arabidopsis plants were grown as described (Schmid et al., 2012). For DR5::SV40:3×GFP seeds, the plates were supplemented with kanamycin (AppliChem, Darmstadt, Germany) to a final concentration of 50 µg/ml. Glufosinate (Plüss-Staufer, Oftringen, Switzerland) was sprayed onto plants carrying the DR5::NLS:tdTomato transgene on the third and sixth day after transfer to soil at a final concentration of 0.2 g/l.

Maize inbred lines A188 and H99 and transgenic lines (Gallavotti et al., 2008) were grown under standard greenhouse conditions at 26°C with 16 hours of light and a relative air humidity of ~60%.

Microscopy and image acquisition

Ovules of *Arabidopsis* plants at various stages were dissected and studied either cleared for 5-15 minutes with 1 M glycine (pH 9.6) solution (as in Fig. 6H-J,M,O) or untreated in water (all other images). The pictures were taken with a Leica SP2 laser-scanning confocal microscope (Leica Microsystems AG, Heerbrugg, Switzerland). The GFP fluorescence was collected at wavelengths of 501-532 nm. For simultaneous YFP and tdTomato imaging, scanning was performed sequentially. Emission light of 503-575 nm and 575-632 nm was collected for the yellow and red channels, respectively. An excitation beam splitter DD 488/543 was used in both cases. Image capture was performed using Leica Confocal Software 2.61 and channel overlay was performed using a custom MATLAB script.

Maize cobs were harvested from greenhouse-grown plants. Whole cobs were treated as described (Srilunchang et al., 2010). For microscopy analyses, ovaries were dissected after clearing, mounted in methyl salicylate, and analysed with an LSM 510-META confocal laser-scanning microscope (Carl Zeiss Microscopy GmbH, Oberkochen, Germany) with 488 nm excitation and a LP 505 filter. For selective ZmPIN1a::PIN1a:YFP visualisation, 514 nm excitation and a BP 530-600 filter were applied, whereas DR5::mRFP:ER fluorescence was observed with 543 nm excitation in combination with a BP 560-615 filter. Image capture and processing were performed using the Zeiss LSM 510 META software and Zeiss LSM Image Browser version 3.5.0.359.

Note added in proof

While our manuscript was under revision, Ceccatto and colleages (Ceccatto et al., 2013) also reported the absence of DR5 activity in the *Arabidopsis* FG.

Acknowledgements

We thank Dolf Weijers (Wageningen University), Jiří Friml (Flanders Institute of Biotechnology), Wei-Cai Yang (Chinese Academy of Science), Markus Geisler (Université de Fribourg) and Cristina Dal Bosco (Albert-Ludwigs-Universität Freiburg) for seeds; Célia Baroux and Christof Eichenberger (University of Zürich) for advice on confocal microscopy; Marc Schmid (University of Zürich) for allowing us to cite unpublished data; Pierre Barbier de Reuille (University of Berne), Enrico Martinoia (University of Zürich), Leah Edelstein-Keshet (University of British Columbia) and Markus Geisler for discussion; and Lucia Colombo (Universita degli Studi di Milano) for critical comments on the manuscript.

Competing interests

The authors declare no competing financial interests

Author contributions

D.S.L. developed and simulated the mathematical models; D.S.L. and N.G.K. conducted experimental studies in *Arabidopsis* and maize, respectively; B.M. and D.J. provided materials; B.H. provided expertise for modeling; T.D. initiated and supervised the maize experiments; U.G. conceived and supervised the project; D.S.L. and U.G. wrote the manuscript, with input from all authors.

Funding

This work was supported by the Universities of Zürich and Regensburg, a postgraduate scholarship (Coordenação de Aperfeiçoamento de Pessoal de Nível Superior-CAPES-Brasília/Brazil) to N.G.K, and an iPhD Project of SystemsX.ch, the Swiss Initiative in Systems Biology to U.G., B.H. and B.M.

Supplementary material

Supplementary material available online at
http://dev.biologists.org/lookup/suppl/doi:10.1242/dev.098301/-/DC1

References

Alon, U. (2007). *An Introduction to Systems Biology: Design Principles of Biological Circuits*, pp. 15. Boca Raton, FL: Chapman & Hall/CRC.

Bent, A. (2006). Arabidopsis thaliana floral dip transformation method. *Methods Mol. Biol.* **343**, 87-103.

Chavarría-Krauser, A. and Ptashnyk, M. (2010). Homogenization of long-range auxin transport in plant tissues. *Nonlinear Anal. Real World Appl.* **11**, 4524-4532.

Christensen, C. A., King, E. J., Jordan, J. R. and Drews, G. N. (1997). Megagametogenesis in Arabidopsis wild type and the Gf mutant. *Sex. Plant Reprod.* **10**, 49-64.

Ceccato, L., Masiero, S., Sinha Roy, D., Bencivenga, S., Roig-Villanova, I., Ditengou, F.A., Palme, K., Simon, R., and Colombo, L. (2013). Maternal control of PIN1 is required for female gametophyte development in Arabidopsis. *PLoS ONE* **8**, e66148.

Curtis, M. D. and Grossniklaus, U. (2003). A gateway cloning vector set for high-throughput functional analysis of genes *in planta*. *Plant Physiol.* **133**, 462-469.

Dal Bosco, C., Dovzhenko, A., Liu, X., Woerner, N., Rensch, T., Eismann, M., Eimer, S., Hegermann, J., Paponov, I. A., Ruperti, B. et al. (2012). The

endoplasmic reticulum localized PIN8 is a pollen specific auxin carrier involved in intracellular auxin homeostasis. *Plant J.* **71**, 860-870.
de Lachapelle, A. M. and Bergmann, S. (2010). Precision and scaling in morphogen gradient read-out. *Mol. Systems Biol.* **6,** 351.
Delbarre, A., Muller, P., Imhoff, V. and Guern, J. (1996). Comparison of mechanisms controlling uptake and accumulation of 2,4-dichlorophenoxy acetic acid, naphthalene-1-acetic acid, and indole-3-acetic acid in suspension-cultured tobacco cells. *Planta* **198**, 532-541.
Desfeux, C., Clough, S. J. and Bent, A. F. (2000). Female reproductive tissues are the primary target of *Agrobacterium*-mediated transformation by the Arabidopsis floral-dip method. *Plant Physiol.* **123**, 895-904.
Escobar-Restrepo, J.-M., Huck, N., Kessler, S., Gagliardini, V., Gheyselinck, J., Yang, W.-C. and Grossniklaus, U. (2007). The FERONIA receptor-like kinase mediates male-female interactions during pollen tube reception. *Science* **317**, 656-660.
Evans, M. M. S. (2007). The indeterminate gametophyte1 gene of maize encodes a LOB domain protein required for embryo Sac and leaf development. *Plant Cell* **19**, 46-62.
Gallavotti, A., Yang, Y., Schmidt, R. J. and Jackson, D. (2008). The relationship between auxin transport and maize branching. *Plant Physiol.* **147**, 1913-1923.
Gallie, D. R. (2002). The 5′-leader of tobacco mosaic virus promotes translation through enhanced recruitment of eIF4F. *Nucleic Acids Res.* **30**, 3401-3411.
Garnett, P., Steinacher, A., Stepney, S., Clayton, R. and Leyser, O. (2010). Computer simulation: the imaginary friend of auxin transport biology. *BioEssays* **32**, 828-835.
Geisler, M., Blakeslee, J. J., Bouchard, R., Lee, O. R., Vincenzetti, V., Bandyopadhyay, A., Titapiwatanakun, B., Peer, W. A., Bailly, A., Richards, E. L. et al. (2005). Cellular efflux of auxin catalyzed by the Arabidopsis MDR/PGP transporter AtPGP1. *Plant J.* **44**, 179-194.
Gregor, T., Bialek, W., de Ruyter van Steveninck, R. R., Tank, D. W. and Wieschaus, E. F. (2005). Diffusion and scaling during early embryonic pattern formation. *Proc. Natl. Acad. Sci. USA* **102**, 18403-18407.
Grieneisen, V. A., Xu, J., Maree, A. F. M., Hogeweg, P. and Scheres, B. (2007). Auxin transport is sufficient to generate a maximum and gradient guiding root growth. *Nature* **449**, 1008-1013.
Gross-Hardt, R., Kägi, C., Baumann, N., Moore, J. M., Baskar, R., Gagliano, W. B., Jürgens, G. and Grossniklaus, U. (2007). LACHESIS restricts gametic cell fate in the female gametophyte of Arabidopsis. *PLoS Biol.* **5**, e47.
Guilfoyle, T. J. and Hagen, G. (2007). Auxin response factors. *Curr. Opin. Plant Biol.* **10**, 453-460.
Gutknecht, J. and Walter, A. (1980). Transport of auxin (indoleacetic acid) through lipid bilayer membranes. *J. Membr. Biol.* **56**, 65-72.
He, F., Saunders, T. E., Wen, Y., Cheung, D., Jiao, R., Rein ten Wolde, P., Howard, M. and Ma, J. (2010). Shaping a morphogen gradient for positional precision. *Biophys. J.* **99**, 697-707.
Huang, B. Q. and Sheridan, W. F. (1994). Female gametophyte development in maize: microtubular organization and embryo sac polarity. *Plant Cell* **6**, 845-861.
Johnston, A. J., Kirioukhova, O., Barrell, P. J., Rutten, T., Moore, J. M., Baskar, R., Grossniklaus, U. and Gruissem, W. (2010). Dosage-sensitive function of retinoblastoma related and convergent epigenetic control are required during the Arabidopsis life cycle. *PLoS Genet.* **6**, e1000988.
Krohn, N. G., Lausser, A., Juranić, M. and Dresselhaus, T. (2012). Egg cell signaling by the secreted peptide ZmEAL1 controls antipodal cell fate. *Dev. Cell* **23**, 219-225.
Lander, A. D., Lo, W.-C., Nie, Q. and Wan, F. Y. (2009). The measure of success: constraints, objectives, and tradeoffs in morphogen-mediated patterning. *Cold Spring Harb. Perspect. Biol.* **1**, a002022.
Liu, J., Mehdi, S., Topping, J., Tarkowski, P. and Lindsey, K. (2010). Modelling and experimental analysis of hormonal crosstalk in *Arabidopsis*. *Mol. Syst. Biol.* **6**, 373.
Ljung, K., Ostin, A., Lioussanne, L. and Sandberg, G. (2001). Developmental regulation of indole-3-acetic acid turnover in Scots pine seedlings. *Plant Physiol.* **125**, 464-475.
Marchant, A., Kargul, J., May, S. T., Muller, P., Delbarre, A., Perrot-Rechenmann, C. and Bennett, M. J. (1999). AUX1 regulates root gravitropism in Arabidopsis by facilitating auxin uptake within root apical tissues. *EMBO J.* **18**, 2066-2073.
Moll, C., von Lyncker, L., Zimmermann, S., Kägi, C., Baumann, N., Twell, D., Grossniklaus, U. and Gross-Hardt, R. (2008). CLO/GFA1 and ATO are novel regulators of gametic cell fate in plants. *Plant J.* **56**, 913-921.
Mori, Y., Jilkine, A. and Edelstein-Keshet, L. (2008). Wave-pinning and cell polarity from a bistable reaction-diffusion system. *Biophys. J.* **94**, 3684-3697.
Ottenschläger, I., Wolff, P., Wolverton, C., Bhalerao, R. P., Sandberg, G., Ishikawa, H., Evans, M. and Palme, K. (2003). Gravity-regulated differential auxin transport from columella to lateral root cap cells. *Proc. Natl. Acad. Sci. USA* **100**, 2987-2991.
Pagnussat, G. C., Yu, H.-J. and Sundaresan, V. (2007). Cell-fate switch of synergid to egg cell in Arabidopsis eostre mutant embryo sacs arises from misexpression of the BEL1-like homeodomain gene BLH1. *Plant Cell* **19**, 3578-3592.
Pagnussat, G. C., Alandete-Saez, M., Bowman, J. L. and Sundaresan, V. (2009). Auxin-dependent patterning and gamete specification in the Arabidopsis female gametophyte. *Science* **324**, 1684-1689.
Petrásek, J. and Friml, J. (2009). Auxin transport routes in plant development. *Development* **136**, 2675-2688.
Ramos, J. A., Zenser, N., Leyser, O. and Callis, J. (2001). Rapid degradation of auxin/indoleacetic acid proteins requires conserved amino acids of domain II and is proteasome dependent. *Plant Cell* **13**, 2349-2360.
Rapparini, F., Tam, Y. Y. Y., Cohen, J. D. and Slovin, J. P. (2002). Indole-3-acetic acid metabolism in *Lemna gibba* undergoes dynamic changes in response to growth temperature. *Plant Physiol.* **128**, 1410-1416.
Rotman, N., Durbarry, A., Wardle, A., Yang, W. C., Chaboud, A., Faure, J. E., Berger, F. and Twell, D. (2005). A novel class of MYB factors controls sperm-cell formation in plants. *Curr. Biol.* **15**, 244-248.
Sbalzarini, I. F., Mezzacasa, A., Helenius, A. and Koumoutsakos, P. (2005). Effects of organelle shape on fluorescence recovery after photobleaching. *Biophys. J.* **89**, 1482-1492.
Schmid, M. W., Schmidt, A., Klostermeier, U. C., Barann, M., Rosenstiel, P. and Grossniklaus, U. (2012). A powerful method for transcriptional profiling of specific cell types in eukaryotes: laser-assisted microdissection and RNA sequencing. *PLoS ONE* **7**, e29685.
Schneitz, K., Hülskamp, M. and Pruitt, R. E. (1995). Wild-type ovule development in Arabidopsis thaliana: a light microscope study of cleared whole-mount tissue. *Plant J.* **7**, 731-749.
Sequeira, L. and Mineo, L. (1966). Partial purification and kinetics of indoleacetic acid oxidase from tobacco roots. *Plant Physiol.* **41**, 1200-1208.
Shaner, N. C., Campbell, R. E., Steinbach, P. A., Giepmans, B. N. G., Palmer, A. E. and Tsien, R. Y. (2004). Improved monomeric red, orange and yellow fluorescent proteins derived from Discosoma sp. red fluorescent protein. *Nat. Biotechnol.* **22**, 1567-1572.
Srilunchang, K. O., Krohn, N. G. and Dresselhaus, T. (2010). DiSUMO-like DSUL is required for nuclei positioning, cell specification and viability during female gametophyte maturation in maize. *Development* **137**, 333-345.
Sundaresan, V. and Alandete-Saez, M. (2010). Pattern formation in miniature: the female gametophyte of flowering plants. *Development* **137**, 179-189.
Swarup, R. and Péret, B. (2012). AUX/LAX family of auxin influx carriers – an overview. *Front. Plant Sci.* **3**, 225.
Swarup, K., Benková, E., Swarup, R., Casimiro, I., Péret, B., Yang, Y., Parry, G., Nielsen, E., De Smet, I., Vanneste, S. et al. (2008). The auxin influx carrier LAX3 promotes lateral root emergence. *Nat. Cell Biol.* **10**, 946-954.
Tucker, M. R., Okada, T., Johnson, S. D., Takaiwa, F. and Koltunow, A. M. G. (2012). Sporophytic ovule tissues modulate the initiation and progression of apomixis in Hieracium. *J. Exp. Bot.* **63**, 3229-3241.
Ulmasov, T., Murfett, J., Hagen, G. and Guilfoyle, T. J. (1997). Aux/IAA proteins repress expression of reporter genes containing natural and highly active synthetic auxin response elements. *Plant Cell* **9**, 1963-1971.
Vernoux, T., Brunoud, G., Farcot, E., Morin, V., Van den Daele, H., Legrand, J., Oliva, M., Das, P., Larrieu, A., Wells, D. et al. (2011). The auxin signalling network translates dynamic input into robust patterning at the shoot apex. *Mol. Syst. Biol.* **7**, 508.
Weijers, D., Schlereth, A., Ehrismann, J. S., Schwank, G., Kientz, M. and Jürgens, G. (2006). Auxin triggers transient local signaling for cell specification in Arabidopsis embryogenesis. *Dev. Cell* **10**, 265-270.
Xiang, C., Han, P., Lutziger, I., Wang, K. and Oliver, D. J. (1999). A mini binary vector series for plant transformation. *Plant Mol. Biol.* **40**, 711-717.
Xu, T., Wen, M., Nagawa, S., Fu, Y., Chen, J.G., Wu, M.J., Perrot-Rechenmann, C., Friml, J., Jones, A.M., and Yang, Z. (2010). Cell surface- and Rho GTPase-based auxin signaling controls cellular interdigitation in Arabidopsis. *Cell* **143**, 99-110.
Yanagisawa, S. and Sheen, J. (1998). Involvement of maize Dof zinc finger proteins in tissue-specific and light-regulated gene expression. *Plant Cell* **10**, 75-89.
Yang, Y., Hammes, U. Z., Taylor, C. G., Schachtman, D. P. and Nielsen, E. (2006). High-affinity auxin transport by the AUX1 influx carrier protein. *Curr. Biol.* **16**, 1123-1127.